*J. Fluid Mech.* (1994), *vol.* 263, *pp.* 185–205



# Trajectories of charged tracer particles around a charged sphere in a simple shear flow

By A. S. DUKHIN† AND T. G. M. VAN DE VEN

Paprican and Department of Chemistry, Pulp and Paper Research Centre, McGill University, Montreal, Canada H3A 2A7

(Received 1 December 1992 and in revised form 13 September 1993)

The trajectories of electrically charged tracer particles travelling around a charged sphere subjected to a simple shear flow have been calculated. This is a limiting case of the relative trajectories of two unequal-sized spheres when the radius ratio $a_1/a_2$ approaches zero. Until now these trajectories have been calculated by assuming the additivity of hydrodynamic and electrostatic forces, while neglecting the electroviscous coupling forces. These electroviscous forces are long range and can significantly alter the relative trajectories of spheres. When $a_1/a_2 \to 0$, it is found that these trajectories depend on two parameters, $\alpha$ and $\beta$, which depend on the surface charge density of the tracer particle and the sphere. The relative trajectories of charged particles are qualitatively different from those of neutral particles. There exist six intervals of $\alpha$-values for which the trajectories of the tracer particle show different features. Several new types of trajectory appear, besides the open and closed trajectories for neutral particles, which we refer to as uni- and bidirectional infinite length trajectories, uni- and bidirectional finite length trajectories, open returning trajectories, and prolate, oblate and circular closed trajectories. This richness of possible trajectories is the result of three electrokinetic phenomena, affecting particle motion: electro-osmotic slip, electrophoretic and diffusiophoretic motion.

## 1. Introduction

The problem of two-sphere interactions in a simple shear flow has been studied extensively over the past 50 years in the fields of both fluid dynamics and colloid science. These interactions form the basis of our understanding of the behaviour of suspensions of spheres subjected to flow. Despite the numerous theoretical and experimental studies, our knowledge of two-sphere interactions is still incomplete, especially for spheres with an electrical surface charge and for spheres coated with polymer or polyelectrolyte. The main difficulty is that for such systems the hydrodynamic and colloidal forces are not additive, but give rise to coupling forces, which we call electroviscous (van de Ven 1988, 1989) and viscopolymeric (De Witt & van de Ven 1992) forces. In this paper we address the problem of the effect of electroviscous forces on two-sphere interactions in a simple shear flow.

For systems in which the colloidal and hydrodynamic forces are additive, two-sphere interactions in shear are well understood. This applies for instance to two spheres in shear subjected to van der Waals attraction. The relative trajectories of two spheres of arbitrary radius ratio in a linear shear flow (in a Newtonian liquid and for low Reynolds numbers) are given by Kao, Cox & Mason (1977) who generalized earlier work on two-sphere interactions in a simple shear flow by Arp & Mason (1977),

† On leave from Ukrainian Academy of Sciences, Kiev, Ukraine.

Batchelor & Green (1972) and Lin, Lee & Sather (1970). Van der Waals forces can be included in the theory by assuming that these forces only act along the line of sphere centres, which results in an additional term in the relative velocity between the spheres. This was first done by Curtis & Hocking (1970) and the relative trajectories were described by van de Ven & Mason (1976). Other colloidal forces, such as electrostatic forces acting between charged spheres, were included in theory in the same way as van der Waals forces (van de Ven & Mason 1976, 1977; Zeichner & Schowalter 1977; Adler 1981), simply by assuming that hydrodynamic and colloidal forces were additive. The same assumptions were made in the theory of gravity-induced coagulation (Melik & Fogler 1984). However, it was shown by one of us (van de Ven 1988, 1989) that the assumption of additivity is not valid, since the hydrodynamic and electrostatic forces are coupled. This coupling arises from the fact that a fluid containing electrically charged colloidal particles also contains ions (to allow for electroneutrality). These ions are subject to an electric field, arising from the potential difference between the surface of a particle and the bulk of the fluid. When an electric field of strength $E$ is acting on a fluid containing ions it produces a body force per unit volume of magnitude $\rho E$, where $\rho$ is the charge density of the fluid (i.e. the number of charges per unit volume). This body force introduces an additional term in the Stokes equation, thus modifying the hydrodynamic forces and torques. These electroviscous forces can be of long range, because hydrodynamic flow fields can polarize the ionic atmosphere (the electric double layer) which surrounds each particle. For a sphere in a simple shear flow this leads to the appearance of an electric quadrupole moment (Dukhin & van de Ven 1993), the influence of which can be felt far beyond the electric double layer.

In this paper we address a limiting case of the problem of the interaction between two electrically charged spheres in a simple shear flow: a small charged tracer particle interacting with a much larger charged sphere. It is hoped that this limiting case will also provide qualitative insight for large tracer particles, similar to the problem of small tracer particles interacting with a neutral sphere. The streamlines around a sphere, calculated by Cox, Zia & Mason (1968), turned out to be qualitatively similar to the relative trajectories of two spheres of equal size. The theory presented here is a natural extension of the theories by Cox *et al.* (1968) for a neutral sphere, by van de Ven (1988) for streamlines around a charged sphere with a low zeta-potential but for arbitrary ionic strength, and by Dukhin & van de Ven (1993) for the streamlines around a charged sphere with a thin double layer but with arbitrary zeta-potential. Here we will assume that the tracer particle is much smaller than the sphere and that the ionic strength is sufficiently high so that the double layer thickness $\kappa^{-1}$ is much smaller than the radius $a$ of the sphere

$$\tau = \kappa a \gg 1. \tag{1}$$

This condition allows us to make use of thin-double-layer theory (Dukhin & Derjaguin 1974). When condition (1) is satisfied, the various polarization fields (hydrodynamic, electric and concentration fields) arising from the action of the hydrodynamic flow around a sphere are known (Dukhin & van de Ven 1993). These polarization fields determine the intensity of long-range interparticle interactions, which are fundamentally different from the short-range interaction. In the short-range region classical equilibrium surface forces (Derjaguin 1989), are significant. The thickness of this region adjacent to the particle surface is approximately $\kappa^{-1}$. In the long-range zone the classical surface forces are negligible and only non-equilibrium forces caused by double-layer polarization in the hydrodynamic flow act between the particles. The characteristic distance in the long-range zone is the particle radius $a$. In the case of thin double layers (condition (1)), interparticle interactions can be considered separately in

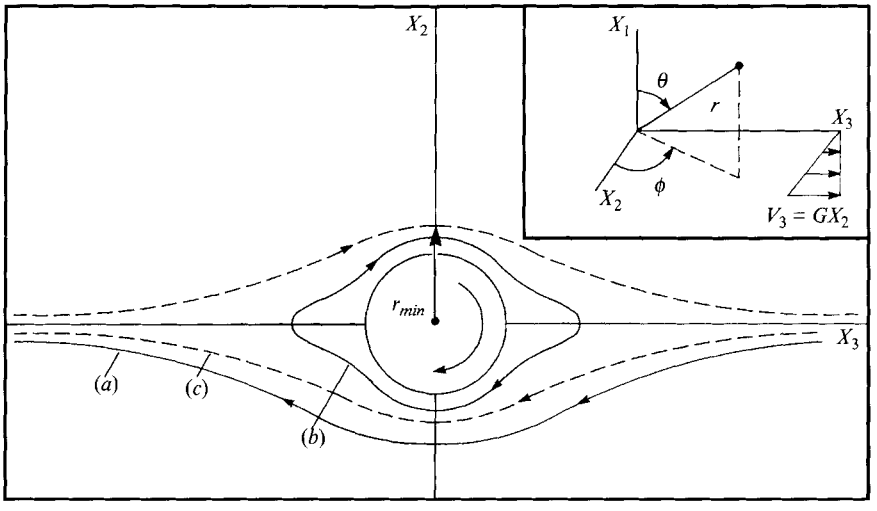


FIGURE 1. Possible trajectories of an uncharged tracer particle around an uncharged sphere in a simple shear flow in the equatorial plane $x_1 = 0$ (schematic): (*a*) an example of an open trajectory, (*b*) of a closed trajectory, while (*c*) represents the limiting trajectory separating open from closed ones; $r_{min}$ is the distance of nearest approach of a tracer particle moving along the limiting trajectory towards the sphere. Inset: $(X_1, X_2, X_3)$ and $(r, \theta, \phi)$ are Cartesian and polar coordinate systems describing the relative position of a tracer particle, represented by a black dot, in a simple shear flow of gradient $G$ with respect to a sphere at the origin.

these two zones. When long-range interactions produced by double-layer polarization in a shear flow are significant, they have to be taken into account when trajectories of interparticle motion are being calculated. Short-range interactions determine only the final stage of the interaction; either particles will aggregate in primary or secondary minima, or aggregation will not occur when the disperse system is stable.

Since we are only considering interactions between small tracer particles and a big sphere, perturbations caused by tracer particles in the polarization fields of the sphere are small and can be neglected.

## 2. Trajectory equations

It is well known that the streamlines around a sphere in a simple shear flow are three-dimensional and can be presented either in a spherical coordinate system $(r, \theta, \phi)$ or in a Cartesian coordinate system $(X_1, X_2, X_3)$ (see inset of figure 1). Possible equatorial streamlines (in plane $X_2, X_3$) around a neutral sphere are shown schematically in figure 1. For small tracer particles, the streamlines are equivalent to their trajectories. Two types of trajectories of tracer particles are possible: open separating trajectories and closed orbits. These two types are separated by a surface of limiting trajectories.

The motion of a charged tracer particle is the result of three different kinds of electrokinetic phenomena. Firstly, electro-osmotic slip in the double layer of the sphere produces a hydrodynamic flow inside the double layer which affects the tracer particles surrounding the sphere. Secondly, an electric field with quadrupole symmetry, originating from the polarization of the double layer in shear flow acts on the charges of the tracer particles, resulting in electrophoretic motion. Thirdly, a concentration field also of quadrupole symmetry, and also caused by the polarization of the double layer in shear flow, acts on the double layers of the tracer particles resulting in diffusiophoresis (Dukhin & Derjaguin 1974).

Quadrupole symmetry of the electric and concentration fields is determined by the rotation of the particle about the $X_1$-axis in shear. The motion of the liquid relative to the surface of the particle caused by its rotation will carry with it the ions in the diffuse part of the double layer. Convective transfer of ions in the diffuse part of the double layer gives rise to a tangential electric current relative to the surface of the particle. The distribution of this surface current was found by Dukhin & van de Ven (1993) using the known velocity profiles. It turned out that in the first and third quadrants of the Cartesian system (cf. figure 1) the current is directed away from the surface, whereas in the second and fourth quadrants it is directed towards the surface. The direction of the radial component of the electric field strength $E_r$ is similar and, consequently, a positive charge is accumulated near the surface in the first and third quadrants and a negative charge in the second and fourth ones. This means that the polarization of the double layer by the hydrodynamic flow results in the emergence of an electric quadrupole moment. The same reasoning can be applied to the concentration field. The quadrupole electric field will carry ions out of the double layer, thus causing electro-osmotic slip.

Therefore the components of the velocity of a tracer particle, in a spherical coordinate system fixed at the centre of the sphere, can be represented as

$$\frac{\mathrm{d}r}{\mathrm{d}t} = G\tilde{A}(r)\sin^2\theta\sin 2\phi + v_{ef}E_r + v_{df}\nabla_r n, \tag{2a}$$

$$r\frac{\mathrm{d}\theta}{dt} = \tfrac{1}{4}Gr\tilde{B}(r)\sin 2\theta\sin 2\phi + v_{ef}E_\theta + v_{df}\nabla_\theta n, \tag{2b}$$

$$r\sin\theta\frac{\mathrm{d}\phi}{\mathrm{d}t} = \tfrac{1}{2}Gr\sin\theta[1+\tilde{B}(r)\cos 2\phi] + v_{ef}E_\phi + v_{df}\nabla_\phi n, \tag{2c}$$

where $v_{ef}$ and $v_{df}$ are the electrophoretic and diffusiophoretic mobilities of the tracer particles, $r$ is the distance between sphere centres, like all other distances rendered dimensionless through division by the sphere radius $a$, and $G$ is the rate of shear. The functions $\tilde{A}(r)$ and $\tilde{B}(r)$ characterize the hydrodynamic flow caused by the electro-osmotic slip in the double layer of the sphere. $E$ and $n$ are the electric and concentration fields, respectively, expressions for which are given by Dukhin & van de Ven (1993). Inserting these expressions in (2) results in

$$\frac{\mathrm{d}r}{\mathrm{d}t} = G\left[A(r)+\frac{3V_2}{r^2G}+\frac{3\alpha}{4r^4}\right]\sin^2\theta\sin 2\phi, \tag{3a}$$

$$\frac{\mathrm{d}\theta}{\mathrm{d}t} = \frac{G}{4}\left[B(r)-\frac{\alpha}{r^5}\right]\sin 2\theta\sin 2\phi, \tag{3b}$$

$$\frac{\mathrm{d}\phi}{\mathrm{d}t} = \tfrac{1}{2}G+\tfrac{1}{2}G\left[B(r)-\frac{\alpha}{r^5}\right]\cos 2\phi. \tag{3c}$$

Here

$$A(r) = \frac{r}{2}-\frac{5}{4r^2}+\frac{2}{4r^4}, \tag{4}$$

$$B(r) = 1-\frac{1}{r^5}, \tag{5}$$

$$\alpha = -\frac{12\Phi_2}{Ga^2}\left[\frac{\epsilon\zeta_s}{\eta}-av_{ef}\right]+\frac{12n_2}{Ga^2}\left[\frac{4\epsilon k^2T^2}{\eta e^2z^2n_0}\ln\cosh\tilde{\zeta}_s-av_{df}\right], \tag{6}$$

and $\Phi_2, n_2, V_2$ are the electric, concentration and hydrodynamic quadrupole moments. The values of these moments depend upon the values of electrokinetic potential, $\zeta_s$, and the Stern potentials, $\psi$, of the sphere and are equal to

$$\Phi_2 = \frac{5kTG}{3\kappa^2 ez}\left[\frac{f^+}{D^+} - \frac{f^-}{D^-}\right], \tag{7}$$

$$n_2 = \frac{5n_0 G}{3\kappa^2}\left[\frac{f^+}{D^+} + \frac{f^-}{D^-}\right], \tag{8}$$

$$V_2 = \frac{12\epsilon k^2 T^2}{\eta a^2 e^2 z^2}\left[\tilde{\zeta}_s \tilde{\Phi}_2 - \frac{n_2}{n_0}\ln\cosh\tilde{\zeta}_s\right], \tag{9}$$

where $k$ is the Boltzmann constant, $T$ the absolute temperature, $D^{\pm}$ are the diffusion coefficients of the positive and negative ions, $\epsilon$ is the dielectric permittivity, $\eta$ the viscosity, $e$ is the charge of a proton, $z$ the valency of the ions, $n_0$ is the bulk electrolyte concentration, $\tilde{\zeta}_s = ez\zeta_s/4kT$, $\tilde{\Phi}_2 = ez\Phi_2/kT$, and the functions $f^{\pm}$ equal

$$f^{\pm} = \frac{\pm\tilde{\zeta}_s + \ln\cosh\tilde{\zeta}_s}{\frac{4}{\tau}[\exp(\mp 2\tilde{\psi}) - 1] + 1}. \tag{10}$$

The above equations are for symmetric electrolytes in which $z_+ = -z_- = z$. The parameter $\alpha$ characterizes the influence of the charge of the tracer particle.

In our analysis we shall follow the paper by Cox *et al.* (1968), devoted to the calculation of trajectories of uncharged tracer particles around an uncharged sphere.

Dividing (3*a*) by (3*b*), and integrating yields

$$\cos\theta = Cf(r), \tag{11}$$

$C$ being an arbitrary constant of integration, and

$$f(r) = [r^3 - [\eta] + \tfrac{3}{2}(1+\alpha)r^{-2}]^{-\frac{1}{3}}, \tag{12}$$

where $[\eta]$ is the intrinsic viscosity of a suspension of charged spheres, given by

$$[\eta] = \tfrac{5}{2} + 6\frac{V_2}{G} = \tfrac{5}{2} + \beta. \tag{13}$$

Similarly dividing (3*c*) by (3*b*) and integrating yields

$$\sin\theta\cos\phi = \pm f(r)[D + (1+\alpha)g(r)]^{\frac{1}{2}}, \tag{14}$$

where $g(r)$ is equal to

$$g(r) = \int_r^{\infty} y^{-3} f(y)\,\mathrm{d}y. \tag{15}$$

Thus we have reached the conclusion that trajectories of charged tracer particles around a charged sphere are described by a set of equations very similar to that for uncharged spheres. In a Cartesian coordinate system these equations may be written in the alternative form

$$x_1 = Crf(r), \tag{16}$$

$$x_2 = \pm rf(r)[D + (1+\alpha)g(r)]^{\frac{1}{2}}, \tag{17}$$

where $C$ and $D$ are constants of integration called trajectory constants, and $f(r)$ and $g(r)$ are defined by (12) and (15).

When the parameters $\beta$ and $\alpha$ are equal zero, the function $f$ reduces to the function for an uncharged sphere and uncharged tracer particle. When $\alpha = 4V_2/G$ and $V_2 \neq 0$, the function $f$ corresponds to the case of trajectories of uncharged tracer particles around a charged sphere. Thus we can consider the influence of the surface charges of tracer particle and sphere on the trajectories by varying the values of the two parameters $\alpha$ and $\beta$ (defined by (6) and (13)). This will be done in the following sections.

## 3. Trajectories of charged tracer particles in the equatorial plane

### 3.1. *General considerations*

Trajectories of tracer particles around a charged sphere in shear flow depend on the surface characteristics of both surfaces – sphere and tracer particle. Hence the trajectory equations contain two parameters $\alpha$ and $\beta$. The parameter $\beta$ characterizes the influence the surface charge of the sphere, whereas $\alpha$ depends on the properties of both surfaces.

The parameter $\beta$ is positive for all $\zeta$-potentials of the sphere. A decrease in the $\zeta$-potential of the sphere leads to a decrease in $\beta$, which equals zero for an uncharged sphere. Realistic values of $\beta$ are much less than 1 since $\beta$ is equal to the magnitude of the primary electroviscous effect: $\beta = [\eta] - \frac{5}{2}$, where $[\eta]$ is the intrinsic viscosity of the suspension.

The range for the parameter $\alpha$ depends on the signs of the $\zeta$-potential of the sphere $\zeta_s$, and of the tracer particle, $\zeta_t$. When the tracer particles are uncharged, $\alpha = \frac{2}{3}\beta$ and, consequently, $\alpha > 0$. When the signs of $\zeta_s$ and $\zeta_t$ are the same, according to (6) an increase in the absolute value of $\zeta_s$ leads to a decrease in $\alpha$. If the electrophoretic and diffusiophoretic mobilities of the tracer particles are sufficiently large, $\alpha$ might be zero or negative. This is the case when $\alpha < \frac{2}{3}\beta$. When the signs of $\zeta_s$ and $\zeta_t$ are opposite, an increase in the absolute value of $\zeta_s$ leads to an increase in $\alpha$. For this case $\alpha > \frac{2}{3}\beta$.

In order to calculate how $\alpha$ depends on the $\zeta$-potential of the tracer particles, the electrophoretic and diffusiophoretic mobilities of the tracer particles have to be known. The thin-double-layer condition (1) might not be valid for a tracer particle because its radius has to be much smaller than the radius of the sphere. Thus a tracer particle is usually not characterized by a thin double layer but by a thick one. In such a case the influence of the relaxation effect on the electrophoretic mobility of a tracer particle is negligible and, according to Helmholtz's theory $v_{ef}$, equals

$$v_{ef} = \frac{2\epsilon\zeta_t}{3\eta a}. \tag{18}$$

The diffusiophoretic mobility of particles with a thick double layer is very small and the influence of this phenomenon on the trajectories of tracer particles can be omitted. Therefore, (6) and (13) can be transformed to the following more convenient form, corresponding to a system of tracer particles with a thick double layer:

$$\beta = \frac{180}{\tau^2}[\tilde{\zeta}_s(m^- f^- - m^+ f^+) + (\ln\cosh\tilde{\zeta}_s)(m^- f^- + m^+ f^+)], \tag{19}$$

$$\alpha = \frac{120}{\tau^2}[(\tilde{\zeta}_s - \tfrac{2}{3}\tilde{\zeta}_t)(m^- f^- - m^+ f^+) + (\ln\cosh\tilde{\zeta}_s)(m^- f^- + m^+ f^+)], \tag{20}$$

where we have introduced the ionic drag coefficients

$$m^{\pm} = \frac{2\epsilon k^2 T^2}{3\eta e^2 z^2 D^{\pm}}. \tag{21}$$

Equations (19) and (20) will be used below to illustrate the general conclusions obtained from a qualitative analysis. A disperse system of colloidal particles suspended in an aqueous KCl solution was chosen as an example. For the electroviscous effect to be considerable, a realistically large value of $\beta$ must be used because a decrease in $\beta$ leads to a decrease in $\alpha$. For this reason the value of $\tau\,(=\kappa a)$ has to be small as possible, while still satisfying condition (1). A good choice is $\tau = 10$, since for smaller values the double layer can no longer be considered thin. The dependence of $\beta$ on $\zeta_s$ shows a maximum in $\beta$ because of the relaxation effect. The maximum value of $\beta$ is achieved when $\zeta \approx 100$ mV for a one-one electrolyte. Higher valencies result in lower values of $\alpha$. The illustrations presented below correspond to this realistic disperse system.

Before discussing the various possible trajectories between charged tracer particles and a charged sphere let us first discuss the shape of the various functions that enter in the trajectory equations. Rewriting (3*a*) as

$$\frac{\mathrm{d}r}{\mathrm{d}t} = \frac{Gh(r)}{2r^2}\sin^2\theta \sin 2\phi \tag{22}$$

shows that the function $h(r) = f(r)^{-3}$ determines whether the velocity of approach or recession is positive or negative. This function $h(r)$ has one extreme point, $r_m$, given by

$$r_m = (1+\alpha)^{\frac{1}{5}} \tag{23}$$

at which the function $h(r)$ equals

$$h(r_m) = [\tfrac{5}{2}(1+\alpha)^{\frac{3}{5}} - \tfrac{5}{2} - \beta]. \tag{24}$$

This extreme value is positive when $\alpha > \alpha^*$, where

$$\alpha^* = (1+\tfrac{2}{5}\beta)^{\frac{5}{3}} - 1$$

and negative when $\alpha < \alpha^*$. When $\alpha < \alpha^*$ two distances appear, $r_1$ and $r_2$, at which $h(r_i) = 0$ (see figure 2). When $\alpha = \frac{2}{3}\beta$, $r_1 = 1$ and for smaller values of $\alpha$, $h(r)$ is zero at only one value of $r$ (i.e. for $r = r_2$). The various shapes of $h(r)$ for different values of $\alpha$ are shown in figure 2 for $\beta = 0.354$. The corresponding function $f(r) = h(r)^{-\frac{1}{3}}$ is also shown for the same range of $\alpha$-values, as is the shape of the function $g(r)$, defined by (15). It can be shown that $g(r)$ remains finite when $f(r_i) = \pm\infty$, by expanding $f(r_i)$ around $r_i$, changing to a new variable $s = r + \epsilon$ and performing the integral in (15) between the limits $\pm\epsilon$, $\epsilon$ being a small parameter.

Besides the critical values $\alpha^*$ and $\frac{2}{3}\beta$, other critical values of $\alpha$ exist. In the equatorial plane ($x = 0$, $C = 0$) all trajectories are coplanar. The tangential velocity $\mathrm{d}\phi/\mathrm{d}t$ can change sign when the absolute value of $\alpha$ is more than 1. This can be seen by considering (3*c*); $\mathrm{d}\phi/\mathrm{d}t$ becomes zero when equation

$$1 + \left(1 - \frac{1+\alpha}{r^5}\right)\cos 2\phi = 0 \tag{25}$$

has at least one solution. This condition is satisfied when $|\alpha| \geqslant 1$. Hence one can expect qualitatively different trajectories for $|\alpha| > 1$ as compared to $|\alpha| < 1$ and thus $\alpha = \pm 1$ are also critical values of $\alpha$.

A final critical value can be obtained by considering the minimum distance of

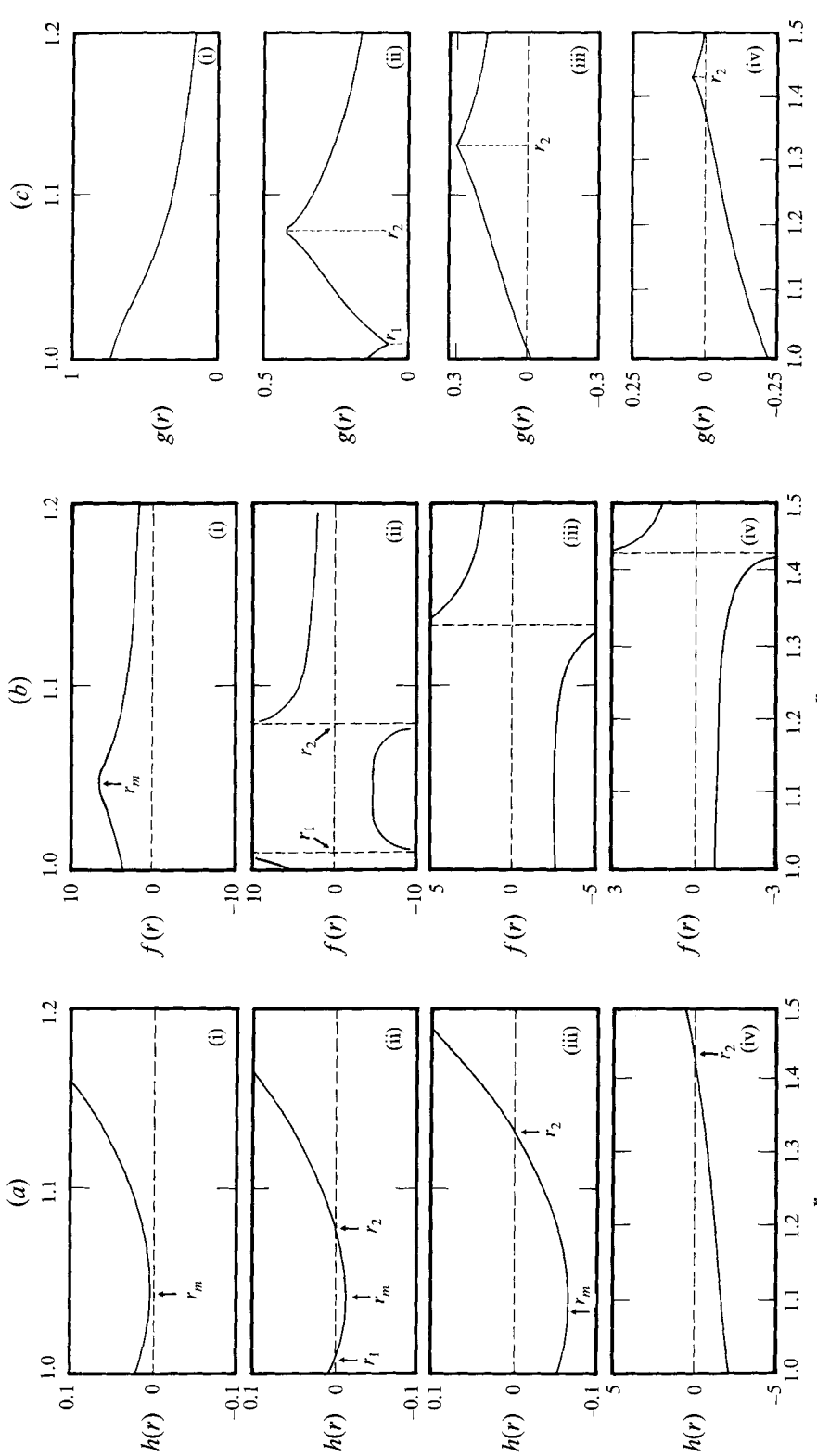


FIGURE 2. Graphs of the functions (*a*) $h(r)$, (*b*) $f(r)$ and (*c*) $g(r)$ for various values of $\alpha$ for a disperse system suspended in an aqueous KCl solution, $\tau = 10$, $\zeta = 100$ mV, $\beta = 0.354$. (i) An example of interval $\alpha > \alpha^*$ ($\alpha = 0.25$); (ii) an example of interval $\alpha^* > \alpha > \frac{2}{3}\beta$ ($\alpha = 0.24$); (iii) an example of interval $\frac{2}{3}\beta > \alpha > -1$ ($\alpha = 0.2$); (iv) an example of interval $\alpha < -1$ ($\alpha = -1.1$). The coordinate of the minimum value of $h(r)$ is denoted as $r_m$ and the roots as $r_1$ and $r_2$. For (i–iii) $1 < r < 1.2$, while for (iv) $1 < r < 1.5$.

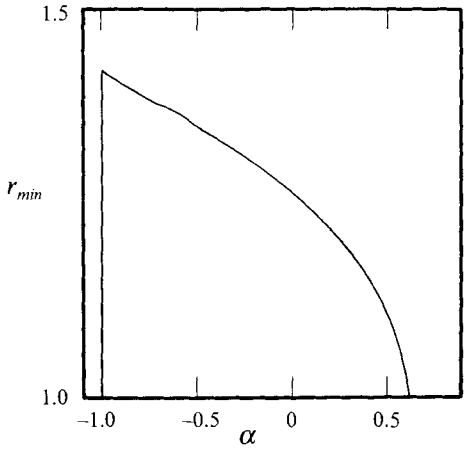


FIGURE 3. The dependence of $r_{min}$ on $\alpha$ for $\beta = 0.354$.

approach a tracer particle can have when approaching the sphere from infinity. This limiting approach distance is reached when the particle travels on the limiting trajectory separating open from closed trajectories (see figure 1). This follows directly from (11) and (14). The closest approach is in the equatorial plane $C = 0$, and if $D > 0$ closed orbits are impossible when $(1+\alpha)g(r) > 0$. Thus this limiting trajectory is characterized by the trajectory constants $C = D = 0$ and thus its trajectory equation is

$$\cos\phi = \pm f(r)[(1+\alpha)g(r)]^{\frac{1}{2}}. \tag{26}$$

The minimum distance of approach is reached when $\phi = 0$ and thus $r_{min}$ satisfies the equation

$$\frac{1}{f(r_{min})^2} - (1+\alpha)g(r_{min}) = 0. \tag{27}$$

The dependence of $r_{min}$ on $\alpha$ has been calculated for $\beta = 0.354$ and the results are shown in figure 3. It can be seen that $r_{min}$ decreases with increasing $\alpha$ and for some value, $\alpha_0$, becomes equal to one. For $\beta = 0.354$ it is found that $\alpha_0 = 0.63$. For values of $\alpha > \alpha_0$ closed trajectories are impossible because the value of $r_{min}$ becomes less than one, which is physically impossible. The reason for the decrease of $r_{min}$ with increasing $\alpha$ is related to the two mechanisms of particle motion. The first mechanism is the motion of particles by hydrodynamic flow, induced by electro-osmotic slip in the double layer of the sphere. The second mechanism is electrokinetic transport in the electric field. If the signs of the $\zeta$-potentials of the sphere and tracer particles are the same, these two mechanisms will move particles into opposite directions, because electrophoretic and electro-osmotic velocities of equally charged surfaces have an opposite sign. The first mechanism causes repulsion of the tracer particles from the sphere. The magnitude of this repulsion is characterized by the value of $\beta$ and increases with an increase in $\beta$. The parameter $\alpha$ characterizes the second mechanism which causes tracer particle attraction to the sphere because its effect goes in the opposite direction. Consequently, for constant $\beta$, $r_{min}$ has to decrease when $\alpha$ increases because the electrophoretic attraction compensates at least partially for the effect of hydrodynamic repulsion. This trend is reflected in figure 3.

The effect of electrophoretic attraction disappears for uncharged tracer particles for which $\alpha = \frac{2}{3}\beta$. In this case an increase in $\beta$ must lead to an increase in $r_{min}$. The

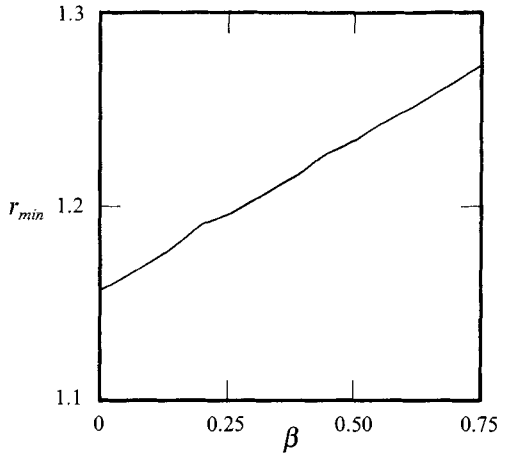


FIGURE 4. The dependence of $r_{min}$ on $\beta$ for uncharged tracer particles suspended in aqueous KCl ($\tau = 10$ and $\alpha = \frac{2}{3}\beta$).

| Case | $\alpha$-interval | Comments |
|---|---|---|
| (i) | $\alpha > 1$ | $d\phi/dt$ changes sign; 2 stagnation points |
| (ii) | $\alpha_0 < \alpha < 1$ | Closed trajectories impossible |
| (iii) | $\alpha^* < \alpha < \alpha_0$ | Closed trajectories possible |
| (iv) | $\frac{2}{3}\beta < \alpha < \alpha^*$ | $dr/dt = 0$ at $r = r_1$ and $r = r_2$ |
| (v) | $-1 < \alpha < \frac{2}{3}\beta$ | $dr/dt = 0$ at $r = r_2$ |
| (vi) | $\alpha < -1$ | $d\phi/dt$ changes sign; 4 stagnation points |

TABLE 1. Various cases of relative trajectories of charged tracer particles and a charged sphere ($\beta = 0.354$) in simple shear

numerical solution of (27) confirms this qualitative conclusion. The dependence of $r_{min}$ on $\beta$ obtained numerically is plotted in figure 4. It can be seen that $r_{min}$ increases linearly with $\beta$. It was shown earlier (van de Ven 1988) that $r_{min}$ increases linearly with $\zeta^2$ for low potentials. Since for low potentials $\beta \propto \zeta^2$, the present results are in agreement with the previous study and show that this linear increase extends well beyond the condition of low potentials.

From the above discussion it can be seen that there exist a number of critical values of $\alpha$, i.e. $\alpha = 1$, $\alpha_0$, $\alpha^*$, $\frac{2}{3}\beta$ and $-1$, from which one can expect that the interactions of tracer particles with a sphere will depend on the interval in which $\alpha$ lies. Qualitative different trajectories are expected for the various intervals. The various cases that are possible are summarized in table 1.

### 3.2. *Specific examples*

*Case* (i) $\alpha > 1$

This case corresponds to high $\zeta$-potentials of the tracer particle. The minimum values of $\zeta_t$, determined by the condition $\alpha = 1$, are given in table 2 for two disperse systems. It can be seen that this case is realized only for extremely high charged particles. However, although rare, the existence of a disperse system with $\alpha > 1$ is not forbidden by any physical law. Also, the primary electroviscous effect becomes larger at smaller values of $\kappa a$. Although the thin-double-layer theory then no longer applies, qualitatively similar effects are expected.

| | | | | | |
|---|---|---|---|---|---|
| KCl | $\alpha = 1$ | $\alpha_0 = 0.63$ | $\alpha^* = 0.245$ | $\alpha = \frac{2}{3}\beta = 0.236$ | $\alpha = -1$ |
| $\beta = 0.354$ | −412 | −214 | −80 | 0 | 658 |
| $LiHCO_3$ | $\alpha = 1$ | $\alpha_0 = 0.945$ | $\alpha^* = 0.478$ | $\alpha = \frac{2}{3}\beta = 0.44$ | $\alpha = -1$ |
| $\beta = 0.66$ | −221 | −201 | −43 | 0 | 462 |

TABLE 2. Values of $\zeta$-potentials of tracer particles (in mV) corresponding to the critical values of $\alpha$ ($\alpha = \pm 1, \alpha_0, \frac{2}{3}\beta, \alpha^*$) for disperse system with $\tau = 10$ and $\zeta_s = 100$ mV suspended in a solution of either KCl ($m^{\pm} = 0.184$) or $LiHCO_3$ ($m^+ = 0.35$, $m^- = 0.338$)

When $\alpha > 1$, the radial velocity component $dr/dt$ is always positive in the first quadrant ($0 < \phi < \frac{1}{2}\pi$). This can be concluded from (29) and the shape of the function $h(r)$ for $\alpha > 1$. However, $d\phi/dt$ can become negative for low values of $\phi$ and small distances of separation. Equation (25) determines the curve at which $d\phi/dt = 0$. For the positions of tracer particles between this curve and the sphere, $d\phi/dt < 0$. The maximum value $r$ on this limiting curve ($r_{cr}$) corresponds to $\phi = 0$ and is equal to

$$r_{cr} = [\tfrac{1}{2}(1+\alpha)]^{\frac{1}{5}}. \tag{28}$$

The points with coordinates $\phi = 0$ or $\phi = \pi$ and $r = r_{cr}$ are stagnation points because both components of the particle velocity are zero. These points are located on a limiting trajectory separating two kinds of trajectories. Trajectories lying outside this trajectory are characterized by positive values of $dr/dt$ and $d\phi/dt$ everywhere. These trajectories correspond to the ordinary open trajectories similar to an uncharged sphere (cf. figure 1).

The ordinary closed trajectories presented in figure 1 are impossible when $\alpha > 1$, since $\alpha > \alpha_0$ and $\alpha_0 < 1$. Thus the limiting trajectory containing the stagnation point separates ordinary open trajectories from trajectories of a new kind. This limiting trajectory is characterized by a critical value of the trajectory constant $D$, $D_{cr}$, which can be found from the condition that the stagnation point belongs to the limiting trajectory. As a result we obtain

$$D_{cr} = \frac{1}{f^2(r_{cr})} - (1+\alpha)\, g(r_{cr}). \tag{29}$$

Trajectories of tracer particles around a charged sphere for the case $\alpha > 1$ are plotted schematically in figure 5. We can distinguish four different kinds of trajectory. The first kind are the ordinary open trajectories. They are characterized by the values of $D$ determined by

$$D > D_{cr}. \tag{30}$$

Not all trajectories with $D > D_{cr}$ are, however, open trajectories. A new type of trajectory is possible which occurs when the initial position of the tracer particle is sufficiently close to the sphere. When $D$ is in the interval

$$D^* > D > D_{cr}, \tag{31}$$

where $D^*$ is equal to

$$D^* = \frac{1}{f^2(1)} - (1+\alpha)\, g(1), \tag{32}$$

the trajectory has two branches. One branch is the ordinary open trajectory, the other is located near the sphere and is symmetrical around the $X_2$-axis. The second branch

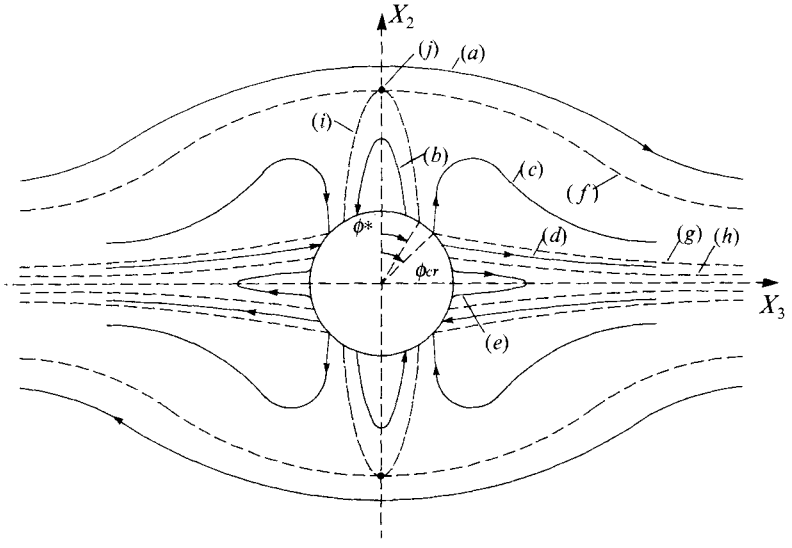


FIGURE 5. Trajectories (schematic) of a charged tracer particle around a charged sphere in a simple shear flow in the equatorial plane ($X_1 = 0$) for $\alpha > 1$: (*a*) an example of an open trajectory, (*b*) of a trajectory of finite length, (*c*) of a bidirectional trajectory, (*d*) of a unidirectional trajectory, (*e*) of a trajectory of finite length symmetrical around the $X_3$-axis, (*f–i*) are the various limiting trajectories, and (*j*) is a stagnation point. The angles $\phi^*$ and $\phi_{cr}$ determine the region where the sources of bidirectional trajectories are located.

of the trajectory starts and ends on the surface of the sphere. We shall refer to this type of trajectory as a 'finite length trajectory' (following Bachelor 1982). Numerical calculation shows that $D^* = 0.409$, $D_{cr} = 0.408$ when $\alpha = 1.1$ and $\beta = 0.354$.

The limiting trajectory characterized by $D_{cr}$ also consists of two branches. The trajectories characterized by values of $D$ less than $D_{cr}$ lie inside the first branch of this limiting trajectory and outside the second branch. All these trajectories contain at least one point of the sphere surface. This point can either be a source or a sink. If the source of a trajectory is located on the sphere between the angles $\phi^* < \phi < \phi_{cr}$, where

$$\cos\phi^* = f(1)\,[D_{cr} + (1+\alpha)\,g(1)]^{\frac{1}{2}}, \tag{33}$$

$$\cos 2\phi_{cr} = 1/\alpha, \tag{34}$$

the tangential component of the velocity of the tracer particle changes direction on this trajectory (cf. (25)). These trajectories will be called 'bidirectional'. This type of trajectory is separated from one side by the limiting trajectory with constant $D_{cr}$ and from the other side by a limiting trajectory with constant $D_f$, given by

$$D_f = \frac{\cos\phi_{cr}}{f^2(1)} - (1+\alpha)\,g(1). \tag{35}$$

Thus the bidirectional (infinite length) trajectories are characterized by values of $D$ in the interval

$$D_{cr} > D > D_f, \tag{36}$$

where $D_f = 0.301$ when $\alpha = 1.1$ and $\beta = 0.354$.

When $D$ is less than $D_f$, $\mathrm{d}\phi/\mathrm{d}t$ does not change sign. This type of trajectory we call 'unidirectional'. According to trajectory equation (14), the length of trajectories characterized by positive values of $D$ is infinite when $g(r) > 0$ (as is the case here). Thus

unidirectional trajectories of infinite length are characterized by values of $D$ in the interval

$$D_f > D > 0. \tag{37}$$

The last type of trajectory is one of finite length symmetrical around the $X_3$-axis. These trajectories are characterized by negative values of $D$ in the interval $D_1 < D < 0$, where

$$D_1 = -(1+\alpha)g(1). \tag{38}$$

The shape of the trajectories presented in figure 5 reflects the balance of the hydrodynamic and electrodynamic factors of particle interaction. In the region near the $X_2$-axis the charged tracer may move against the flow along a trajectory of finite length. Thus in this region the combination of electrophoretic and electro-osmotic motion is stronger than the purely hydrodynamic interaction. The intensities of these factors are equal at the stagnation points.

However, the region where the electrodynamical factor predominates is much smaller than the region where the hydrodynamic factor is stronger. Nevertheless, the influence of the electrodynamical interaction is strong enough and causes qualitative changes in the trajectories, such as an absence of ordinary closed trajectories.

It is also important to mention that the electrodynamical interaction might lead to deposition of the tracer particles. In the case of uncharged particles there is no deposition according to the classical analysis. Charged tracer particles deposit on the surface of the large particle in the second and fourth quadrants and near the $X_2$-axis (see figure 5).

The decrease of the electrokinetic potential reduces the importance of the electrodynamical interaction, as shown in the following examples.

*Case* (ii) $\alpha_0 < \alpha < 1$

A decrease in $\alpha$ leads to a decrease in $\phi_{cr}$ and $\phi^*$. When $\alpha$ becomes equal to 1, both $\phi_{cr}$ and $\phi^*$ become equal to zero. As a result, bidirectional trajectories transform into unidirectional trajectories and unidirectional ones symmetrical about the $X_2$-axis disappear. In the range $\alpha_0 < \alpha < 1$ there are three types of trajectory, as shown schematically in figure 6. The shape of the unidirectional trajectories is determined by the fact that $\mathrm{d}r/\mathrm{d}t$ is zero when $\phi = \frac{1}{2}n\pi$. Since $\alpha > \alpha_0$ no closed orbits exist.

Open trajectories are separated from unidirectional (infinite length) ones by a limiting trajectory passing through the point ($r = 1$, $\phi = 0$), which is consequently characterized by the trajectory constant $D^*$. Hence open trajectories are characterized by $D > D^*$ ($D^* = 0.073$ when $\alpha = 0.7$ and $\beta = 0.354$), unidirectional trajectories by $0 < D < D^*$ and finite-length trajectories by $D_1 < D < 0$.

The decrease of the electrokinetic potential causes the decay of the electrodynamical interaction. In this case the hydrodynamics predominate everywhere because the direction of the particle motion coincides with the direction of the flow in each point. However, the electrodynamical interaction is still strong enough to eliminate the closed trajectories. As a result, the possibility of tracer particle deposition remains in this range of electrokinetic potentials. It can also be seen that the trajectories reflect the quadrupole symmetry of the interaction.

*Case* (iii) $\alpha^* < \alpha < \alpha_0$

If the value of $\alpha$ becomes less than $\alpha_0$, ordinary closed trajectories appear because $r_{min}$ becomes greater than 1. Thus in this interval if $\alpha$-values there are three types of trajectory, shown schematically in figure 7. Positive values of $D$ correspond to open

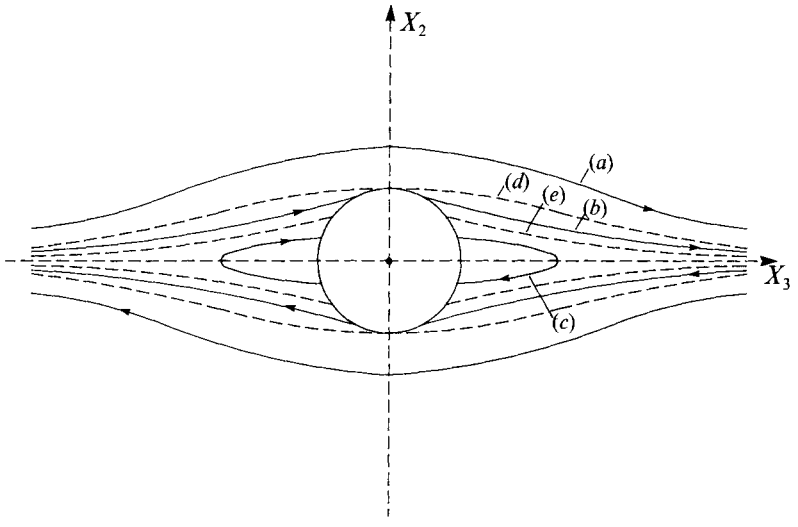


FIGURE 6. Trajectories (schematic) of a charged tracer particle around a charged sphere in a simple shear flow in the equatorial plane ($X_1 = 0$) for $\alpha_0 < \alpha < 1$. Trajectory (*a*) is an example of an open trajectory, (*b*) of a unidirectional trajectory, (*c*) of a trajectory of finite length, (*d*, *e*) are the limiting trajectories.

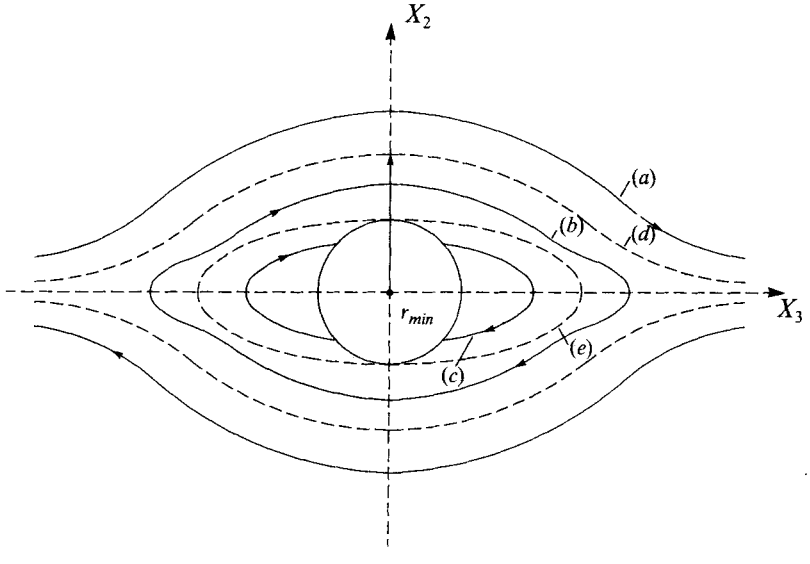


FIGURE 7. Trajectories (schematic) of a charged tracer particle around a charged sphere in a simple shear flow in the equatorial plane ($X_1 = 0$) for $\alpha^* < \alpha < \alpha_0'$: (*a*) an example of an open trajectory, (*b*) of a closed trajectory, (*c*) of a trajectory of finite length, (*d*, *e*) correspond to the limiting trajectories.

trajectories. Values of $D$ in the interval $D^* < D < 0$ correspond to the closed trajectories. Values of $D$ in the interval $D_1 < D < D^*$ correspond to trajectories of finite length. For $\alpha = 0.4$ and $\beta = 0.354$ the trajectory constants of finite-length trajectories lie in the interval $-0.709 < D < -0.316$.

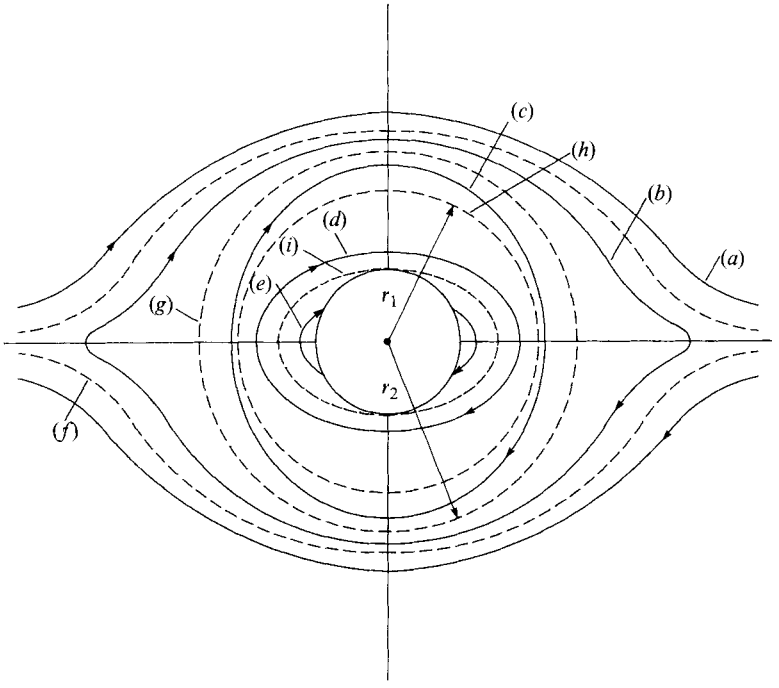


FIGURE 8. Trajectories (schematic) of a charged tracer particle around a charged sphere in a simple shear flow in the equatorial plane for $\frac{2}{3}\beta < \alpha < \alpha^*$: (*a*) an example of an open trajectory, (*b*) of a closed prolate trajectory, (*c*) of a closed oblate trajectory, (*d*) of an internal closed prolate trajectory, (*e*) of a trajectory of finite length $r_1$ and $r_2$ are the radii of the circle which separate closed prolate trajectories from closed oblate ones; (*f–i*) are limiting trajectories.

*Case* (iv) $\frac{2}{3}\beta < \alpha < \alpha^*$

If the value of $\alpha$ becomes less than $\alpha^* = [(1+\frac{2}{5}\beta)^{\frac{5}{3}} - 1]$, new types of trajectories appear because in this case the radial component of the velocity, $\mathrm{d}r/\mathrm{d}t$, can change sign in the first quadrant. When the value of $\alpha$ is in the interval $\frac{2}{3}\beta < \alpha < \alpha^*$, the function $h(r)$ has two zero points with coordinates $r_1$ and $r_2$. In the interval between these two zero points, the function $h(r)$ is negative and thus $\mathrm{d}r/\mathrm{d}t$ is negative in the first quadrant. This means that two new limiting trajectories have appeared. These trajectories are circles of radius $r_1$ and $r_2$, respectively. Closed trajectories located between these two circles have an oblate shape because $X_2^{max} > X_3^{max}$ ($X_i^{max}$ being the maximum distance of separation in the $i$-direction).

Thus in this case there are four types of trajectory, shown schematically in figure 8: open, closed prolate, closed oblate and finite-length trajectories. $D > 0$ corresponds to the usual open trajectories, $-(1+\alpha)g(r_2) < D < 0$ corresponds to closed prolate trajectories, $-(1+\alpha)g(r_2) < D < -(1+\alpha)g(r_1)$ corresponds to the closed oblate trajectories, $D^* < D < -(1+\alpha)g(r_1)$ corresponds to a second set of closed prolate orbits, while $D_1 < D < D^*$ corresponds to finite-length trajectories.

*Case* (v) $-1 < \alpha < \frac{2}{3}\beta$

A decrease in $\alpha$ leads to a decrease in the radius of the inner circular trajectory. When $\alpha$ becomes equal to $\frac{2}{3}\beta$ (uncharged tracers around a charged sphere), the inner circle disappears. The trajectories for smaller values of $\alpha$, i.e. for the interval $-1 < \alpha < \frac{2}{3}\beta$, are presented schematically in figure 9. It can be seen that closed oblate and finite-

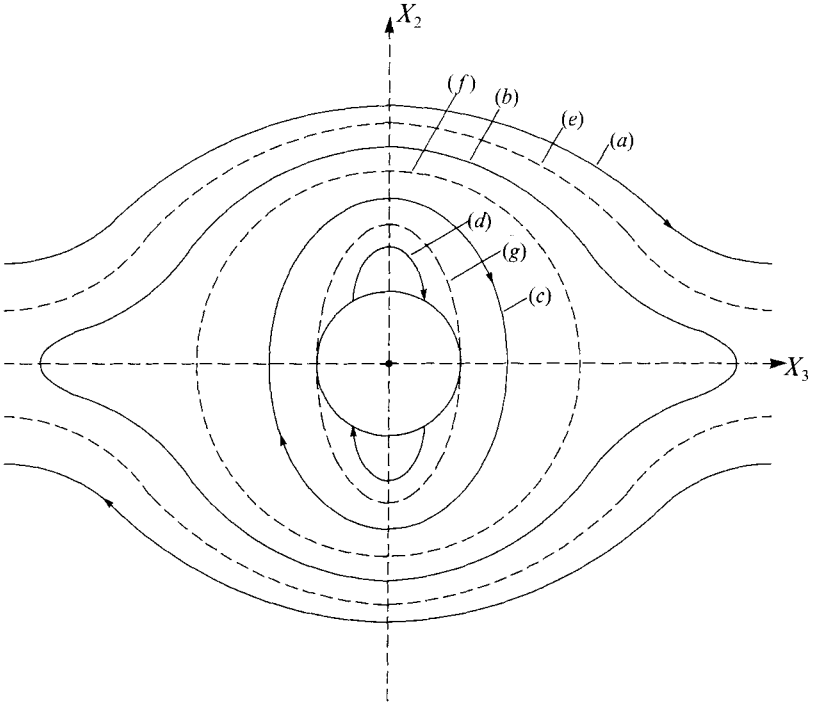


FIGURE 9. Trajectories (schematic) of a charged tracer particle around a charged sphere in a simple shear flow in the equatorial plane for $-1 < \alpha < \frac{2}{3}\beta$: (*a*) an example of an open trajectory, (*b*) of a closed prolate trajectory, (*c*) of a closed oblate trajectory, (*d*) of a trajectory of finite length, (*e–g*) correspond to the limiting trajectories.

length trajectories are located inside the circle of radius $r_2$. The finite-length trajectories have shifted to $\phi = 0, \pi$. The limiting trajectory separating trajectories of finite length from closed ones passed through the point ($r = 1$, $\phi = \frac{1}{2}\pi$). The trajectory constant of this limiting trajectory, $D_1$, equals $-(1+\alpha)g(1)$ and, according to figure 2, is positive.

As in the previous case, $D > 0$ corresponds to open trajectories and

$$-(1+\alpha)g(r_2) < D < 0$$

corresponds to closed prolate trajectories ($D = -(1+\alpha)g(r_2)$ being the circular trajectory). The oblate closed orbits are characterized by

$$-(1+\alpha)g(r_2) < D < D_1,$$

while the finite-length trajectories correspond to $D_1 < D < D^*$. The case $\alpha = \beta = 0$ (neutral tracer particles around a neutral sphere) is a limiting case of this range of $\alpha$-values, where $r_2 = 1$ and no oblate closed orbit nor finite-length trajectories exist.

*Case* (vi) $\alpha < -1$

When $\alpha$ approaches the value of $-1$ (but $\alpha > -1$), the time it takes for a tracer particle to complete (half) a closed orbit approaches infinity. When $\alpha = -1$, tracer particles can no longer cross the $X_3$-axis when moving along a closed orbit, which indicates the disappearance of closed orbits. Thus the trajectories for $\alpha < -1$ are quantitatively different from those with $\alpha > -1$. Besides the disappearance of closed orbits, several stagnation points appear. According to (34) and (25), the curve at which

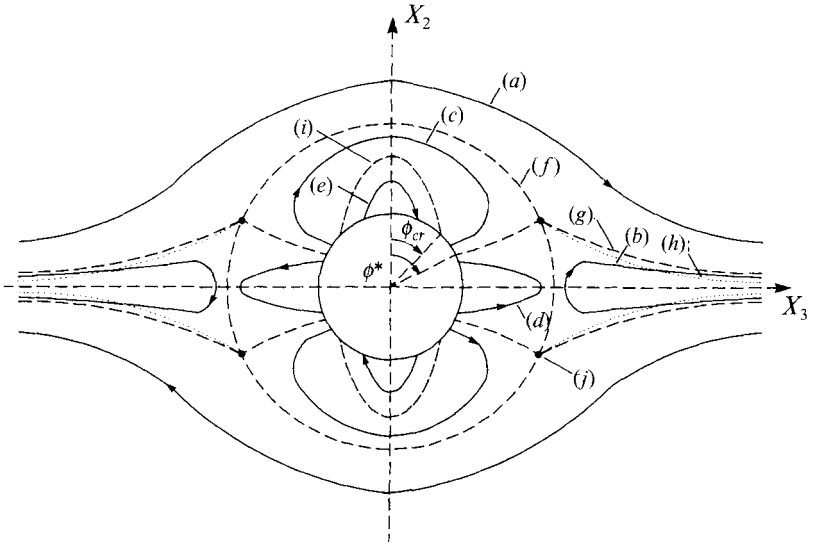


FIGURE 10. Trajectories (schematic) of a charged tracer particle around a charged sphere in a simple shear flow in the equatorial plane for $\alpha < -1$: (*a*) an example of an open trajectory, (*b*) of a returning trajectory, (*c*) of a bidirectional trajectory of finite length, (*d*) of a unidirectional trajectory of finite length, (*e*) of a unidirectional trajectory of finite length symmetrical around the $X_2$-axis, (*f*, *g–i*) correspond to the limiting trajectories, (*h*) to the line where $\mathrm{d}\phi/\mathrm{d}t$ equals zero, and (*j*) is a stagnation point.

$\mathrm{d}\phi/\mathrm{d}t = 0$ extends to $r = \infty$ when $\alpha < -1$. When this curve intersects with the circle $r = r_2$, for which $\mathrm{d}r/\mathrm{d}t = 0$, we have a stagnation point. Since the curve $\mathrm{d}\phi/\mathrm{d}t$ has four branches, one in each quadrant, four stagnation points appear when $\alpha < -1$. The coordinates of these stagnation points are $(r_2, \phi_s)$, with $\phi_s$ determined by

$$\cos 2\phi_s = -[1-(1+\alpha)/r_2^5]^{-1}. \tag{39}$$

The presence of these stagnation points results in a new type of trajectory which we call open returning trajectories. They are characterized by a tracer particle approaching the sphere from infinity, then turning around and separating towards infinity in the same direction that it came from. This is a result of the large electrodynamic repulsion between the tracer particle and the sphere.

The various trajectories for $\alpha < -1$ are shown in figure 10. It can be seen that we have two types of open trajectories – regular separating trajectories and returning trajectories – and there exist finite-length trajectories. If the source of the finite-length trajectory is located on the sphere in the interval of $\phi$-angles give by $\phi^* < \phi < \phi_{cr}$, with $\phi_{cr}$ given by (34), and $\phi^*$ by

$$\cos\phi^* = f(1)[(1+\alpha)(g(1)-g(r_2))]^{\frac{1}{2}}, \tag{40}$$

The tangential component of velocity of the tracer particles moving along this trajectory changes sign. We will call these trajectories 'bidirectional finite-length trajectories' in order to distinguish them from 'unidirectional finite-length trajectories' characterized by the same sign of $\mathrm{d}\phi/\mathrm{d}t$ at each point of the trajectory.

The various limiting trajectories, i.e. those dividing the open separating trajectories from open returning ones, those dividing open separating trajectories from finite-length trajectories and those dividing the bidirectional trajectories from unidirectional

ones symmetrical about the $X_3$-axis, are all characterized by the same trajectory constant $D_{lim} = -(1+\alpha)\,g(r_2)$. Values of $D > D_{lim}$ can correspond to various types of trajectory depending on the initial position of the tracer particle. The unidirectional finite-length trajectories, symmetrical around $X_2$, are characterized by $D_{lim} < D < D^*$, the bidirectional finite-length trajectories by $D^* < D < D_f$, the unidirectional finite length trajectories, symmetrical around $X_3$, by $D_1 < D < D_{lim}$, and returning trajectories by $D > D_{lim}$.

When $\alpha$ approaches $-1$ (but $\alpha < -1$), $\phi_{cr} \to \pm\frac{1}{2}\pi$, the four stagnation points become two points located at $(r_2, \pm\frac{1}{2}\pi)$, the finite-length trajectories symmetrical around the $X_3$-axis disappear and the finite-length trajectories symmetrical around the $X_2$-axis in quadrants 4 and 1 join those in quadrants 2 and 3. They become the closed oblate trajectories when $\alpha > -1$. The returning trajectories collapse into the $X_3$-axis and disappear, causing some open trajectories to become closed orbit. Hence although the trajectories around the sphere for $\alpha < -1$ look rather different from those for which $\alpha > -1$, a smooth transition between them occur when $\alpha$ passes through $-1$.

We have shown that the trajectories of charged tracer particles around a charged sphere show a surprising richness of possibilities, despite the fact that the trajectory equations appear rather similar to those for uncharged particles. Several new types of trajectory (closed oblate, bi- and unidirectional finite-length, returning, and uni- and bidirectional infinite-length trajectories) have appeared, due to the influence of surface charge. Other new features are the existence of stagnation points for some values of the parameters.

## 4. Three-dimensional trajectories of charged tracer particles

It was shown in the previous section that the surface of a charged sphere rotating in a shear flow contains sources and sinks of trajectories of charged tracer particles. It follows from the analysis of the two-dimensional trajectories in the equatorial plane that tracer particles end up on the equator in the second and the fourth quadrants when $\alpha > \frac{2}{3}\beta$ and in the first and the third quadrants when $\alpha < \frac{2}{3}\beta$.

Analysis of two-dimensional trajectories cannot provide an answer to the question about the stability of the sinks in the equatorial plane. To answer this question the direction of the tangential component of the tracer particle velocity, $\mathrm{d}\theta/\mathrm{d}t$, on the surface of the sphere ($r = 1$) has to be taken into account. According to (3*b*)

$$\mathrm{d}\theta/\mathrm{d}t = -\tfrac{1}{4}G\alpha \sin 2\theta \sin 2\phi. \tag{41}$$

It can be seen that this velocity component has opposite directions for positive and negative values of $\alpha$. Consequently the stability of sinks in the equatorial plane depends on the value of $\alpha$. The condition of stability is governed by the value of $\mathrm{d}\theta/\mathrm{d}t$ when $\theta$ crosses the equatorial plane ($\theta = \frac{1}{2}\pi$). The location in the equatorial plane will be stable if $\mathrm{d}\theta/\mathrm{d}t$ changes sign from positive to negative. In such a case a tracer particle slightly displaced from the equatorial plane will return back to the equator. If the change in $\mathrm{d}\theta/\mathrm{d}t$ is opposite, the position on the equator will be unstable and the tracer particles will move to the north pole ($\theta = 0$) or to the south pole ($\theta = \pi$) of the sphere. Depending on the value of $\alpha$, we can distinguish three different cases.

*Case* (i) $\alpha > \frac{2}{3}\beta$

According to the argument above, the location of a tracer particle on the equator is stable in the second and the fourth quadrants. These locations of the tracer particles are shown in figure 11(*a*) by thick solid lines.

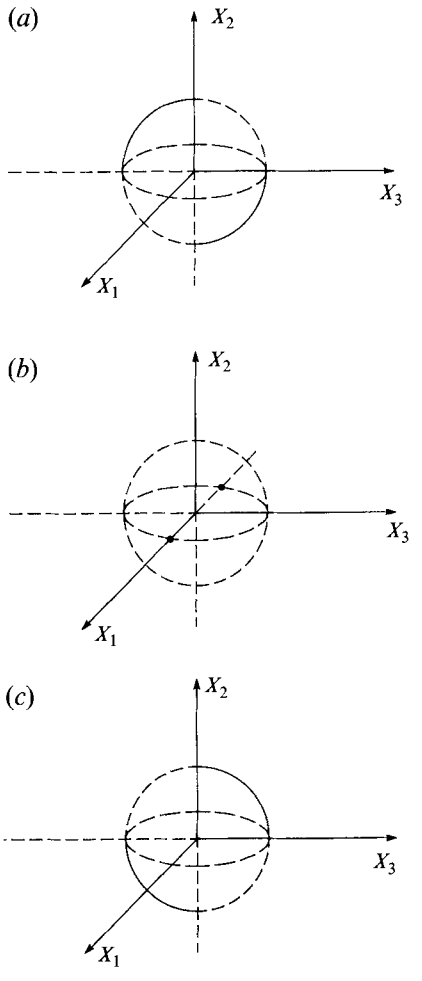


FIGURE 11. Stable locations of charged tracer particles on the surface of a charged sphere in a simple shear flow (schematic), indicated by solid lines or dots. (*a*) $\alpha > \frac{2}{3}\beta$; (*b*) $0 < \alpha < \frac{2}{3}\beta$; (*c*) $\alpha < 0$.

*Case* (ii) $0 < \alpha < \frac{2}{3}\beta$

In this case the location of the tracer particles on the equator is unstable. The tracer particles concentrate at the north and south poles of the sphere, as shown in figure 11(*b*) by solid dots.

*Case* (iii) $\alpha < 0$

The location of the equator is stable in this case, but the tracer particles concentrate on the first and the third quadrants instead of the second and fourth quadrants. This is shown in figure 11(*c*) by thick solid lines.

## 5. Conclusions

The influence of surface charge on the relative trajectories of tracer particles around a sphere subjected to a simple shear flow results in qualitative changes in the nature of the trajectories of the tracer particles compared with uncharged particles. Closed orbits, one of the two types of trajectory of an uncharged tracer particles around an

uncharged sphere, exist only for a limit range of $\zeta$-potentials of the sphere and tracer particles. New types of trajectory for the tracer particles appear, due to the influence of the surface charge. Trajectories of finite length, which start and end on the surface of the sphere, exist because the relative velocity of the tracer particles is not equal to zero on the surface of the charged sphere. Instead, this velocity equals the velocity of electro-osmotic slip in the double layer of the charged sphere.

Trajectories of finite length can be either bidirectional or unidirectional, depending on the sign of the tangential velocity $\mathrm{d}\phi/\mathrm{d}t$. If the sign of $\mathrm{d}\phi/\mathrm{d}t$ does not change along the trajectory of finite length, the trajectory is referred to as unidirectional. Bidirectional trajectories are not likely to be encountered in real systems because they are characterized by an unrealistically high value of the $\zeta$-potential. Bidirectional trajectories exist when $|\alpha| > 1$.

For quite realistic values of the $\zeta$-potentials, closed trajectories can change their shape due to the influence of the surface charge of the sphere and the tracer particles. Ordinary closed trajectories have a prolate shape. But for many realistic values of the $\zeta$-potentials closed trajectories have an oblate shape.

For large negative values of $\alpha$, returning trajectories can exist. But it appears to be almost impossible to prepare disperse systems with high enough $\zeta$-potentials to observe this type of trajectory.

The surface of a charged sphere in a simple shear flow contains sources and sinks of the tracer particles. If the $\zeta$-potential of the tracer particles has a sign opposite to that of the sphere, the tracer particles end up on the equator in the second and the fourth quadrants of a Cartesian coordinate system. If the $\zeta$-potential of the tracer particles has the same sign as that of the sphere, but is less in absolute value, the tracer particles end up on the poles of the sphere. If the $\zeta$-potential of the tracer particles has the same sign as the $\zeta$-potential of the sphere, and is larger in absolute value, the tracer particles end up on the equator of the sphere in the first and the third quadrants.

The equations used to describe the relative motion of the particles do not contain the radius of the tracer particle. A very similar system of equations can be used to describe the relative motion of two spheres of equal size at large separations (i.e. the leading order of an expansion in the small parameter $a/r$, where $a$ is the radius of the sphere). Only the dependence of the parameter $\alpha$ on the $\zeta$-potential will change because $v_{ef}$ will be different. Thus the conclusions obtained in this paper for unequal-sized spheres with $a_1/a_2 \ll 1$ can be applied to monodisperse systems if the distance between particles centres is sufficiently large.

Experimental observations of the types of trajectory described here appear to be difficult. For a large colloidal sphere with a diameter of a few microns, the tracer particle must be a fraction of a micron. Observing such spheres while they are in motion is not easy, but conceivably could be done using a travelling microtube apparatus (Vadas, Goldsmith & Mason 1973). It is, however, much easier to observe these electroviscous effects indirectly, e.g. by measuring the rate of deposition of small particles onto large ones in a simple shear flow. Obviously in this case the short-range interactions have to be considered as well.

## REFERENCES

ADLER, P. M. 1981 Interaction of unequal spheres. I. Hydrodynamic interaction: colloidal forces. *J. Colloid Interface Sci.* **84**, 461.

ARP, P. A. & MASON, S. G. 1977 The kinetics of flowing dispersions. VIII. Doublet of rigin spheres. *J. Colloid Interface Sci.* **61**, 21.

BATCHELOR, G. K. 1982 Sedimentation in a dilute polydisperse system of interaction spheres. *J. Fluid Mech.* **119**, 379.

BATCHELOR, G. K. & GREEN, J. T. 1972 The hydrodynamic interaction of two small freely moving spheres in a linear flow field. *J. Fluid Mech.* **56**, 375.

COX, R. G., ZIA, I. Y. Z. & MASON, S. G. 1968 Particle motions in sheared suspensions. XV. Streamlines around cylinders and spheres. *J. Colloid Interface Sci.* **27**, 7.

CURTIS, A. S. G. & HOCKING, L. M. 1970 Collision efficiency of equal spherical particles in a shear flow. *Trans. Faraday Soc.* **66**, 1381.

DERJAGUIN, B. V. 1989 *Theory of Stability of Colloids and Thin Films.* New York: Consultants Bureau.

DE WITT, J. A. & VEN, T. G. M. VAN DE 1992 Collisions of polymer-coated colloidal spheres in a linear shear flow. *J. Colloid Interface Sci.* **151**, 118.

DUKHIN, S. S. & DERJAGUIN, B. V. 1974 Electrokinetic phenomena. In *Surface and Colloid Science* (ed. E. Matijevic), vol. 7. Wiley.

DUKHIN, A. S. & VEN, T. G. M. VAN DE 1993 A spherical particle surrounded by a thin double layer in a simple shear flow. *J. Colloid Interface Sci.* **158**, 85.

KAO, S. V., COX, R. G. & MASON, S. G. 1977 Streamlines around single spheres and trajectories of pairs of spheres in two-dimensional creeping flows. *Chem. Engng Sci.* **32**, 1505.

LIN, C. J., LEE, K. J. & SATHER, N. F. 1970 Slow motion of two spheres in shear flow. *J. Fluid Mech.* **43**, 35.

MELIK, C. H. & FOGLER, H. S. 1984 Gravity-induced flocculation. *J. Colloid Interface Sci.* **101**, 72.

VADAS, E. B., GOLDSMITH, H. L. & MASON, S. G. 1973 The microrheology of colloidal dispersions. I. The microtube technique. *J. Colloid Interface Sci.* **43**, 630.

VEN, T. G. M. VAN DE 1988 Streamlines around a charged sphere in shear flow. *PhysicoChem. Hydrodyn.* **10**, 97.

VEN, T. G. M. VAN DE 1989 *Colloid Hydrodynamics*, p. 366. Academic.

VEN, T. G. M. VAN DE & MASON, S. G. 1976 The microrheology of colloidal dispersions. IV. Pairs of interacting spheres in shear flow. *J. Colloid Interface Sci.* **57**, 505.

VEN, T. G. M. VAN DE & MASON, S. G. 1976 The microrheology of colloidal dispersions. VII. Orthokinetic doublet formation of spheres. *Colloid Polymer Sci.* **255**, 468.

ZEICHNER, G. R. & SCHOWALTER, W. R. 1977 Use of trajectory analysis to study stability of colloidal dispersions in shear flow. *AIChE J.* **23**, 243.